Texture and chemical composition analyses on the $Hg_{0.66}Pb_{0.33}Ba_2Ca_2Cu_3O_y$ superconductor using the sealed quartz tube technique

J. C. L. Chow and P. C. W. Fung
Physics Department and Centre for Materials Science, University of Hong Kong, Hong Kong

H. M. Shao
Physics Department, National Laboratory of Solid State Microstructure, Nanjing University, Nanjing 210008, China

C. C. Lam
Department of Physics and Materials Science, City University of Hong Kong, Hong Kong

(Received 24 February 1995; accepted 14 December 1995)

Pb-substituted Hg-based superconductor of $Hg_{0.66}Pb_{0.33}Ba_2Ca_2Cu_3O_y$ has been fabricated using the sealed quartz tube technique. *R-T* and x-ray diffraction pattern (XDP) measurements show that the specimen has a T_c of 135 K and contains mainly the Hg-1223 phase. Scanning electron microscopy/energy dispersive x-ray analysis (SEM/EDX) and transmission electron microscopy/energy dispersive x-ray analysis (TEM/EDX) were employed to study the texture and chemical composition of the specimen. It is found that the specimen contains round-shaped grains with a mixture of Hg-1223, $BaCuO_2$, and $Ca_{0.85}CuO_2$ phases, square-shaped grains with a formula of $PbBa_2O_3$, small single crystals with single Hg-1223 phase, and crystal-like layers with a mixture of Hg-1223 and $BaCuO_2$ phase. We consider that though the doping of Pb can benefit the stabilization of the Hg-1223 phase, it introduces other impurity phases and textures in the specimen at the same time.

I. INTRODUCTION

Since the discovery of the high temperature superconductivity in the Hg-1201, Hg-1212, and Hg-1223 ceramics with transition temperatures T_c = 96, 120, and 135 K, respectively,[1–7] researchers have tried to find a feasible but rather standard fabrication method in order to produce a high quality Hg-based superconductor (which may have different phases) with high superconducting phase content. The difficulty of searching for a suitable way to fabricate this family of superconductors is that Hg vapor can easily be produced during the solid-state reaction process. We know that in the mechanism of growing Hg-based superconducting phase compounds, Hg-containing compounds such as HgO are highly volatile at temperatures above their melting point of 500 °C.[8,9] The generation of Hg vapor during the sintering process at 750 °C causes two problems. Firstly, Hg vapor is extremely toxic. It is highly dangerous to fabricate such superconductors in an open environment without proper safety procedures. Secondly, since the Hg-1223 superconducting phase formation temperature of Hg-based superconductors is around 750 °C, HgO in the specimen being fabricated will be decomposed into oxygen and mercury vapor at 500 °C before reaching the superconducting phase formation temperature.

In order to prevent severe Hg loss during the fabrication process, there are two methods that are commonly employed to fabricate the Hg-based superconductors. They are the "high-pressure synthesis"[3,6] and the "sealed quartz tube technique".[10–12] The use of high-pressure synthesis technique can lower the amount of mercury oxide loss. Therefore, scientists sinter the specimen under a high pressure ~2 GPa. The stability of $HgCaO_2$, which is formed at the first stage of the phase formation reaction, can be reduced. This reduction benefits the formation of Hg-based superconducting compounds because the formation of $HgCaO_2$ inhibits the Hg superconducting phase to grow. On the other hand, in sealed quartz tube technique, the specimen is sintered inside a closed environment. The Hg vapor and the O_2 gas, which are decomposed from the specimen at 500 °C, impose a very high vapor pressure on the closed environment of the quartz tube. Therefore, the tube should be first evacuated ($\sim 10^{-2}$ Torr) in order to prevent it from breaking during the sintering process because of the high magnitude of Hg and O_2 vapor pressure. The Hg vapor enters the specimen inside the sealed tube at the Hg-superconducting phase formation temperature of 750 °C and has the chance to react with other chemical constituents and form the Hg superconducting phase.

In general, both the high pressure and sealed quartz tube technique can produce Hg superconductors with very high critical temperature.[3,6,10,13] However, only the sealed quartz tube technique is suitable for preparing

more than one or two pellets. The encapsulation process is likely to be suitable and simple to synthesis the Hg-based superconductors.[4,5] In this paper, the specimen is fabricated by using the encapsulation technique.

Since the superconducting phase formation mechanism of Hg-based superconductors as mentioned above is quite different from that of the typical Y, Bi, and Tl based superconductors, it is fruitful to investigate the texture and to understand the relationships among the phase growth mechanism, the final chemical compositions, the texture geometry, the arrangements, and the shapes of different kinds of grains in the Hg-based superconductors. In order to study these relationships, a Pb-substituted Hg-based superconductor with a stoichiometric formula of $Hg_{0.66}Pb_{0.33}Ba_2Ca_2Cu_3O_y$ was fabricated according to the sintering procedure of Ref. 14. The reason for substituting Pb into the superconductor is because Pb-doping leads to the stabilization of the Hg-1223 structure.[9,15-18] Moreover, it is found that the textures of the specimen contain round-shaped and square-shaped grains, small single crystals, and layers. All of them have different chemical compositions. This interesting phenomenon, which is different from the typical textures of the melt-textured and polycrystalline YBCO superconductors,[19-21] will be discussed in Secs. III and IV.

II. EXPERIMENTAL

Analytical reagent (A. R.) grade chemical powders of HgO (99%), BaO (99%), CaO (99%), and CuO (99%) were weighted and mixed according to the stoichiometric formula of $Hg_{0.66}Pb_{0.33}Ba_2Ca_2Cu_3O_y$. The BaO and CaO were obtained by decomposing pure $CaCO_3$ and $BaCO_3$ (>99.5%) in a vacuum furnace at 950–1000 °C for 6 h and 24 h, respectively. The mixed powders were ground to fine grains 1 μm in size inside a dry box. The use of the dry box is to prevent CO_2 and moisture in the atmosphere from being absorbed by the powder mixture. The finished mixtures were pressed into a rectangular bar of $2 \times 4 \times 20$ mm^3. The specimen was then wrapped in silver foil and placed on a quartz tube. The tube was annealed in a preheated tube furnace at 715–725 °C for 3–4 min. Then the specimen was taken out, ground, pressed again into bar, and reannealed at the same temperature and time. This procedure was repeated four times in order to produce a mixture of precursor $Ba_2Ca_2Cu_3O_x$ and the HgO oxide.[14] After this step, the specimen was wrapped again with silver foil and then encapsulated in a quartz tube, which was evacuated to a pressure of $\sim 10^{-2}$ Torr. The quartz tube was sintered at 750 °C for 10 h and rapidly cooled to room temperature in about 3 min. The specimen was then taken out and annealed at 300 °C for 8 h in flowing oxygen.

The resistance-temperature relationship was measured by a standard four-probe technique using the avalanche photodiode (APD) characterization system. The XDP with Cu K_α radiation of the specimen was characterized by the Siemen's D5000 x-ray diffractometer. Moreover, the Cambridge S360 scanning electron microscope and the JEOL JEM 2000 FX transmission electron microscope in which both, equipped with the energy dispersive x-ray analysis system with model Link-eXL, were employed to investigate the texture, microstructure, and chemical composition of the specimen.

III. RESULTS AND DISCUSSIONS

The resistance-temperature relationship is shown in Fig. 1. The specimen undergoes a superconducting transition with a $T_c \sim 135$ K, which is the critical temperature of the Hg-1223 superconducting phase. The XDP measurement was done on the surface of the sample, as shown in Fig. 2. Almost all of the x-ray diffraction peaks of the specimen can be identified to be the Hg-1223 phase having a tetragonal unit cell ($P4/mmm$). The lattice parameters of the Hg-1223 phase in the specimen are found to be $a = b = 3.852$ Å and $c = 15.861$ Å.

Figure 3 is a typical SEM micrograph showing the fracture surface of the specimen. In the figure, it is found that the specimen contains certain clusters of small square-shaped grains which are distributed everywhere in the fracture surface of the specimen. Moreover, round-shaped grains are found in the lower right-hand corner of the figure. A single crystal-like grain is found in the middle of the figure. Such a grain, in fact, can be found in other positions of the specimen and will be discussed in Fig. 7. On the other hand, the specimen contains a number of single crystal-like layers with curved steps. These different textures of the specimen together with their chemical compositions found by

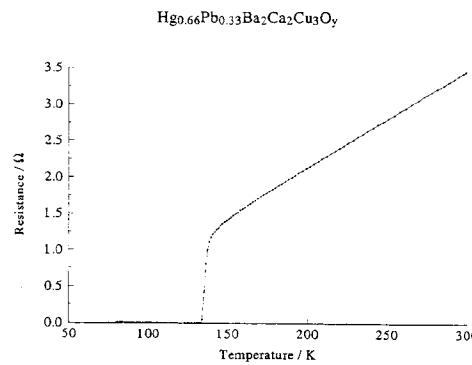

FIG. 1. Resistance-temperature relationship of the $Hg_{0.66}Pb_{0.33}Ba_2Ca_2Cu_3O_y$ superconductor.

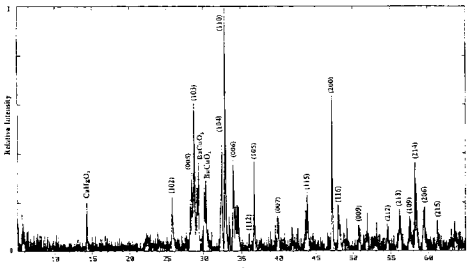

FIG. 2. X-ray diffraction pattern of the $Hg_{0.66}Pb_{0.33}Ba_2Ca_2Cu_3O_y$ superconductor.

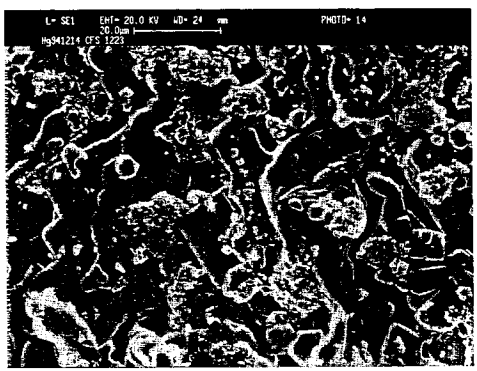

FIG. 3. SEM micrograph showing the fracture surface of the $Hg_{0.66}Pb_{0.33}Ba_2Ca_2Cu_3O_y$ superconductor.

energy dispersive x-ray analysis (EDX) will be discussed in Figs. 5–8. Figure 4 shows the TEM micrograph of the specimen with a magnification of 1×10^6 times. The lattice fringes in the figure are parallel to the (001) plane of the specimen. The spacing of the fringes is ~15.8 Å, showing that the lattice fringes correspond to the Hg-1223 phase.

In order to investigate the chemical compositions of the square-shaped and round-shaped grains, small single crystal, and the layer structure of the specimen in greater detail, EDX analysis is employed to analyze these textures. Figure 5(a) shows the SEM micrograph of the small square-shaped grains in the specimen with sizes ranging from ~0.5–1 μm. The arrangement and shape of the grains in the layer matrix in the specimen are similar to that observed in the Sn-doped melt-textured YBCO superconductor.[22,23] The small grains in the Sn-doped melt-textured YBCO superconductor consist mainly of Sn atoms and are nonsuperconducting. EDX analysis on the grains in Fig. 5(a) with the resulting spectrum as

FIG. 4. TEM micrograph showing the Hg-1223 lattice fringes of the $Hg_{0.66}Pb_{0.33}Ba_2Ca_2Cu_3O_y$ superconductor.

indicated in Fig. 5(b) shows that the grains have a chemical formula of $PbBa_2O_3$, which is nonsuperconducting. We consider that these grains are impurity phase in the specimen and are formed during the sintering process as Pb is substituted into the specimen.

Figures 6(a) and 6(b) show the SEM micrographs and the EDX spectrum of the round-shaped grains in the specimen, respectively. These grains are typical and can be found in various papers concerning the fabrication of the Hg-1223 superconductors.[9,13,24–26] The results of the average quantitative elemental analyses by EDX over the surface indicated in Fig. 6(a) were Hg : Pb : Ba : Ca : Cu = 0.67 : 0.32 : 2.96 : 3.06 : 4.96. The ratio of Hg and Pb is "reasonable" based on the stoichiometric ratio of the specimen $Hg_{0.66}Pb_{0.33}Ba_2Ca_2Cu_3O_y$. However, these round-shaped grains seem to contain higher order Hg-based phases such as the Hg-1234 and Hg-1245 rather than the Hg-1223 phase. Referring to the *R-T* and XDP results as shown in Figs. 1 and 2, the specimen contains mainly the Hg-1223 phase. In the TEM microstructure analysis, although we have occasionally discovered some Hg-1234 lattice fringes intergrowth between the Hg-1223 fringes, the amount of Hg-1234 phase is too small to be detected by the *R-T* and XDP measurement. Therefore, we consider these

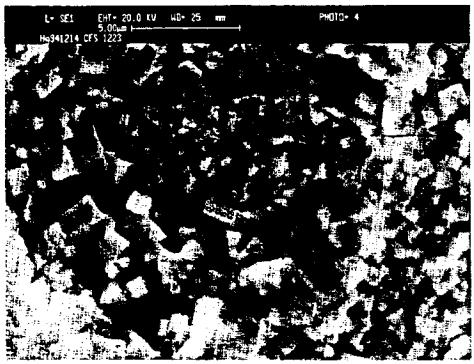

(a)

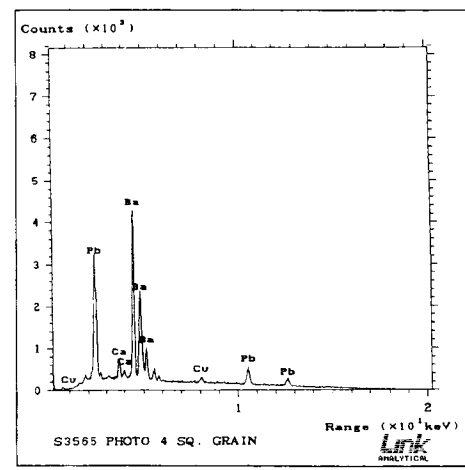

(b)

FIG. 5. (a) SEM micrograph showing the square-shaped grains in the specimen. (b) EDX spectrum of the square-shaped grains in the specimen.

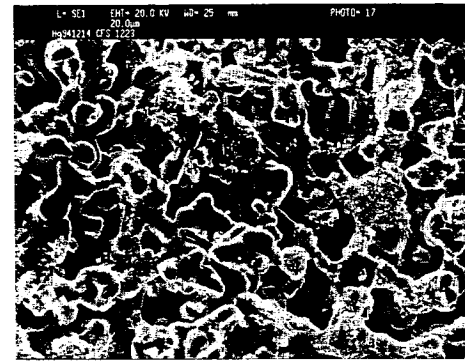

(a)

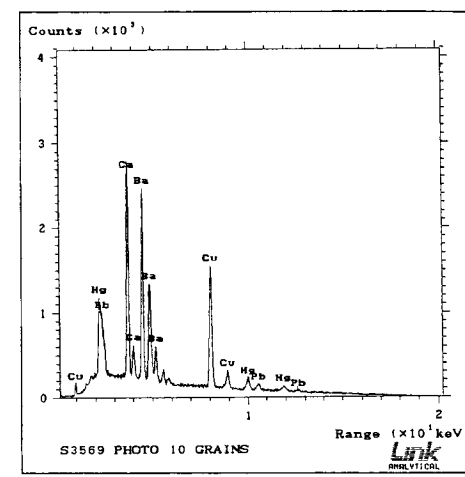

(b)

FIG. 6. (a) SEM micrograph showing the round-shaped grains in the specimen. (b) EDX spectrum of the round-shaped grains in the specimen.

grains to be a mixture of the Hg-1223, $BaCuO_2$, and $Ca_{0.85}CuO_2$ phase [$1335 \approx 1223 + 0101 + 00(0.85)1$]. Since this result has not found in the typical pure Hg-1223 superconductor,[14] it is considered that the formation of the $BaCuO_2$ and $Ca_{0.85}CuO_2$ phase is due to the substitution of Pb in the specimen which affects the superconducting phase formation mechanism.

Figures 7(a) and 7(b) show the SEM micrograph and its corresponding EDX spectrum of a small single crystal in the specimen, respectively. The EDX analysis demonstrates the average quantitative elemental ratios of the crystal Hg : Pb : Ba : Ca : Cu = 0.66 : 0.33 : 1.98 : 2.19 : 3.31. Similar to the analysis of Figs. 6(a) and 6(b), the ratio of Hg and Pb is "reasonable" according to the stoichiometric ratio of the specimen, Hg : Pb = 0.66 : 0.33. The crystal is considered to correspond to the Hg-1223 phase. In fact, in our previous research works regarding the polycrystalline YBCO superconductor,[19] such a small ($\sim$10 μm) crystal can usually be observed in the SEM morphologies. The formation of these crystals reflects that there are some locations in the Hg-specimen during the sintering process where the Hg-1223 crystal growth conditions are suitable.

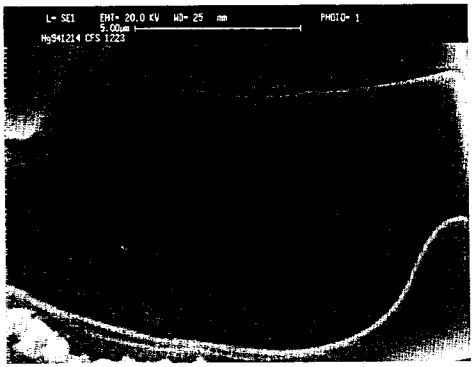

(a)

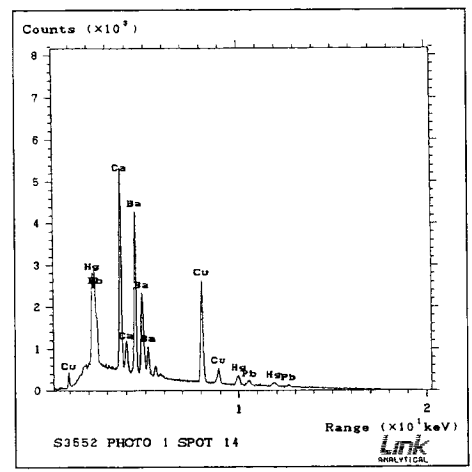

(b)

FIG. 7. (a) SEM micrograph showing a small single crystal in the specimen. (b) EDX spectrum of the small single crystal in the specimen.

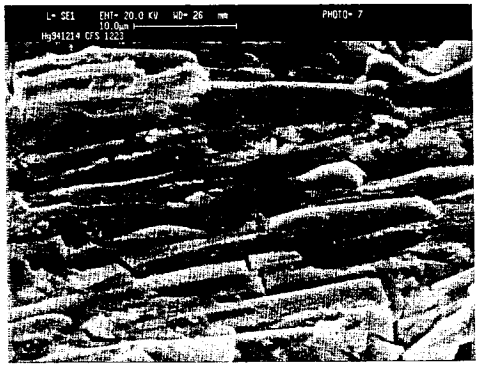

(a)

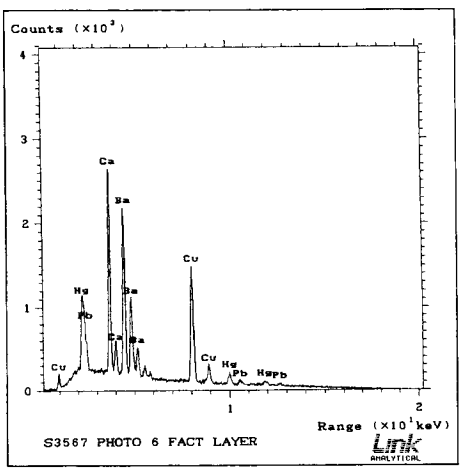

(b)

FIG. 8. (a) SEM micrograph showing the single crystal-like layers structure in the specimen. (b) EDX spectrum of the single crystal-like layers structure in the specimen.

Figures 8(a) and 8(b) are the SEM micrograph and its corresponding EDX spectrum of the layers structure in the specimen, respectively. These crystal-like layers or plate-like crystals can be observed in other papers reporting the fabrication of Hg-1223 superconductors.[14] In Ref. 14, it is found that the atomic ratios of Hg : Ba : Ca : Cu = 1 : 2.24 : 2.26 : 2.92 for a pure phase of the Hg-1223 superconductor using the fabrication procedure similar to this paper. The atomic ratios of the Pb substituted specimen using the EDX analysis in this study were found to be Hg : Pb : Ba : Ca : Cu = 0.69 : 0.31 : 2.07 : 3.14 : 4.16, which suggests the presence of high amount of the Hg-1234 phase. However, based on the *R-T*, XDP, and TEM microstructure analysis results as mentioned above, we consider the layer crystals to be a mixture of the Hg-1223 and $BaCuO_2$ phase. Although the nonsuperconducting $BaCuO_2$ oxide exists in the texture of the specimen, the Hg-1223 phase seems to dominate the superconducting characteristics of the specimen.

Note that the XDP measurement was carried out on the surface while the EDX measurement was carried out on the fractured surface of the sample. Because of the special solid-state reaction of the Hg-superconductor,

the phases identified on the surface of the sample may not be the same as its fractured surface. Therefore, the $CaHgO_2$ phase as shown in Fig. 2 cannot be found in our SEM/EDX measurement, and the $PbBa_2O_3$, $BaCuO_2$, and $Ca_{0.85}CuO_2$ phases detected by the SEM/EDX measurement cannot be found in the XDP of Fig. 2.

IV. CONCLUSION

Although the Pb-substituted specimen demonstrates the superconducting characteristics of the Hg-1223 phase, it is found that the texture of the specimen contains round and square-shaped grains, crystal-like layers, and small single crystals. EDX analyses show that the small single crystals consist of the pure Hg-1223 phase, and the layered structure and the round-shaped grains consist of a mixture of Hg-1223, $BaCuO_2$, and $Ca_{0.85}CuO_2$ phases. Furthermore, we believe the square-shaped grains are found to contain mainly the nonsuperconducting phase of $PbBa_2O_3$ oxide.

At this state, we conclude only that the "special solid-state reaction" of the Hg-1223 superconductor with the substitution of Pb can introduce various grain and crystal textures in the specimen. Each texture has its own chemical compositions that correspond to mainly superconducting Hg-1223 or nonsuperconducting $BaCuO_2$ and $Ca_{0.85}CuO_2$ phases. Although the substitution of Pb can stabilize the formation of the Hg-1223 phase, it can also introduce $BaCuO_2$, and $Ca_{0.85}CuO_2$ oxides, as well as different textures of grains and layers in the specimen.

REFERENCES

1. S. N. Putilin, E. V. Antipov, O. Chmaissem, and M. Marezio, Nature (London) **362**, 226 (1993).
2. A. Schilling, M. Cantoni, J. D. Guo, and H. R. Ott, Nature (London) **363**, 56 (1993).
3. S. N. Putilin, E. V. Antipov, and M. Marezio, Physica C **212**, 266 (1993).
4. M. Itoh, A. Tokiwa-Yamamoto, S. Adachi, and H. Yamauchi, Physica C **212**, 271 (1993).
5. A. Tokiwa-Yamamoto, K. Isawa, M. Itoh, S. Adachi, and H. Yamauchi, Physica C **216**, 250 (1993).
6. M. Hirabayshi, K. Tokiwa, M. Tokumoto, and H. Ihara, Jpn, J. Appl. Phys. **32**, L1206 (1992).
7. Z. J. Huang, R. L. Meng, X. D. Qiu, Y. Y. Sun, J. Kulik, Y. Y. Xue, and C. W. Chu, Physica C **217**, 1 (1993).
8. R. L. Meng, L. Beauvais, X. N. Zhang, Z. J. Huang, Y. Y. Sun, Y. Y. Xue, and C. W. Chu, Physica C **216**, 21 (1993).
9. K. Isawa, A. Tokiwa-Yamamoto, M. Itoh, S. Adachi, and H. Yamauchi, Physica C **217**, 11 (1993).
10. K. Isawa, A. Tokiwa-Yamamoto, M. Itoh, S. Adachi, and H. Yamauchi, Physica C **222**, 33 (1994).
11. O. Chmaissem, L. Wessels, and Z. Z. Sheng, Physica C **230**, 231 (1994).
12. H. M. Shao, C. C. Lam, P. C. W. Fung, X. S. Wu, J. H. Du, G. J. Shen, J. C. L. Chow, S. L. Ho, K. C. Hung, and X. X. Yao, Physica C **246**, 207 (1995).
13. L. Gao, Y. Y. Xue, F. Chen, Q. Xiong, R. L. Meng, D. Ramirez, and C. W. Chu, Phys. Rev. B **50** (6), 4260 (1994).
14. H. M. Shao, L. J. Shen, J. C. Shen, X. Y. Hua, P. F. Yuan, and X. X. Yao, Physica C **232**, 5 (1994).
15. A. Schilling, M. Cantoni, O. Jeandupeux, J. D. Guo, and H. R. Ott, in *Adv. Superconductivity IV*, edited by T. Fujita and Y. Shiohara (Springer, Tokyo, 1994), p. 231.
16. J. Karpinski, H. Schwer, I. Mangelschots, K. Conder, A. Morawski, T. Lada, and A. Paszewin, Physica C **234**, 10 (1994).
17. Z. Iqbal, T. Datta, D. Kirren, A. Lungu, J. C. Barry, F. J. Owens, A. G. Rinzler, D. Yang, and F. Reidinger, Phys. Rev. B **49**, 12322 (1994).
18. Y. Y. Xue, Z. J. Huang, and Z. D. Qiu, Mod. Phys. Lett. B. **7**, 1833 (1993).
19. P. C. W. Fung, J. C. L. Chow, and J. Gao, J. Supercond. **6** (5), 327 (1993).
20. J. C. L. Chow, P. C. W. Fung, Z. L. Du, T. F. Yu, and Y. C. Mok, Cryogenics **34**, 245 (1994).
21. J. C. L. Chow and P. C. W. Fung, Chem. Phys. Lett. **223**, 185 (1994).
22. P. C. W. Fung, Z. L. Du, J. C. L. Chow, Z. H. He, T. F. Yu, Y. Y. Luo, Q. Y. Li, and Y. Lu, Physica C **212**, 279 (1993).
23. Z. L. Du, P. C. W. Fung, J. C. L. Chow, T. F. Yu, Z. H. He, Y. Li, Y. Y. Luo, and J. X. Zhang, Physica C **215**, 319 (1993).
24. O. Chmaissem, Q. Huang, E. V. Antipov, S. N. Putilin, M. Marezio, S. M. Loureiro, J. J. Capponi, J. L. Tholence, and A. Santoro, Physica C **217**, 265 (1993).
25. J. Li, S. Y. Ding, H. M. Shao, J. S. Zhu, and Y. N. Wang, Physica C **232**, 10 (1994).
26. M. Marezio, E. Antipov, J. Copponi, C. Chaillout, S. Loureiro, S. Putilin, A. Santoro, and J. Tholence, Physica B **197**, 570 (1994).